miR-19a/b and MeCP2 repress reciprocally to regulate multidrug resistance in gastric cancer cells

FEI ZHU[*], QIONG WU[*], ZHEN NI[*], CHAO LEI, TING LI and YONGQUAN SHI

State Key Laboratory of Cancer Biology and Institute of Digestive Diseases, Xijing Hospital,
Fourth Military Medical University, Xi'an, Shaanxi 710032, P.R. China

Abstract. Despite the improvement in gastric cancer (GC) treatment, multidrug resistance (MDR) is still a significant reason for chemotherapy failure. Our previous studies have demonstrated that miR-19a/b upregulation directly promoted MDR in GC cells. However, the exact regulation and the potential molecule mechanisms have not been fully clarified. In this study, we found that miR-19a/b was directly involved in 5-aza-2'-deoxycytidine (5-Aza-dC) induced MDR of GC cells. Mechanically, demethylation of miR-19a/b repressed methyl CpG binding protein 2 (MeCP2) expression via direct binding at the 3'-untranslated regions, which then alleviated the inhibitory effects of MeCP2 on miR-19a/b expression. Thus, the mutual regulatory network sustains preservation of the expression levels of miR-19a/b. We further demonstrated that miR-19a/b expression was inversely correlated to MeCP2 expression in GC tissues. These data showed an intimate interplay among miR-19a/b methylation, MeCP2 activity, and MDR, revealing a potential therapeutic target for GC.

Introduction

Gastric cancer (GC) is one of the most common malignant tumors with high morbidity and mortality worldwide, especially in China (1). Despite the improvement in treatment, chemotherapy remains the pivotal strategy for advanced GC. However, multidrug resistance (MDR) is still the most significant reason for chemotherapy failure (2).

MicroRNAs are non-coding 18-24 nucleotide RNA that inhibit the expression of target genes by binding to the 3'-untranslated regions (3'-UTRs). Recently, accumulating evidence has indicated the important role of aberrant miRNAs expression in MDR (3). Moreover, DNA methylation is a critical mechanism in regulating microRNA expression that has been frequently reported in many cancer biological processes, including MDR (2,4).

miR-19a/b belongs to the miR-17-92 cluster and is widely over-expressed in various cancers (5,6). Cancer pathways, such as E2F transcription factors (7), transforming growth factor-β (TGF-β) (8) and c-Myc (9), can interact with the miR-17-92 cluster. Furthermore, previous study indicated that epigenetic modification regulated the expression of miR-17-92 cluster (10). However, whether this methylation of miR-19a/b is involved in MDR of GC and the underlying molecular mechanisms remain unclear.

In the present study, we found that miR-19a/b was directly involved in 5-aza-2'-deoxycytidine (5-Aza-dC) induced MDR of GC cells. Mechanically, methyl CpG binding protein 2 (MeCP2), a member of methyl CpG binding proteins (MBPs), was demonstrated to be a direct target of miR-19a/b. Furthermore, MeCP2 could repress the expression of miR-19a/b in reverse. Lastly, we demonstrated that miR-19a/b expression was inversely correlated to MeCP2 expression in GC tissues.

Materials and methods

Cell line culture and drug treatment. Human GC cell line SGC7901 was obtained from Academy of Military Medical Science (Beijing, China) and maintained in our laboratory. Parental MDR variants SGC7901/VCR and SGC7901/ADR were established and maintained in our laboratory. All the cell lines were cultured in RPMI-1640 medium supplemented with 10% fetal bovine serum (FBS) at 37°C in a humidified atmosphere containing 5% CO_2. For drug treatment, cells were cultured with 5-Aza-dC (2.5 and 4 μM) for 72 h, and then were harvested for the analysis of drug sensitivity, microarray or mRNA expression.

Quantitative RT-PCR. Total RNA was extracted using TRIzol (Invitrogen, Carlsbad, CA, USA), and the concentration of the total RNA was quantified by measuring the absorbance at 260 nm. cDNA was synthesized by reverse transcription according to the manufacturer's instructions (Takara Biotechnology, Dalian, China). Quantitative RT-PCR was performed using SYBR Premix Ex Taq II (Takara Biotechnology) and measured in a LightCycler 480 system

Correspondence to: Professor Yongquan Shi, State Key Laboratory of Cancer Biology and Institute of Digestive Diseases, Xijing Hospital, Fourth Military Medical University, 127 Changlexi Road, Xi'an, Shaanxi 710032, P.R. China
E-mail: shiyquan@fmmu.edu.cn

(Roche, Basel, Switzerland). U6 was used as an internal control. The RNA expression of one sample compared to the calibration sample was calculated using the $2^{-\Delta\Delta CT}$ method. Each experiment was performed in triplicate.

Microarray analysis. Microarray analysis was performed using Agilent Human miRNA (8x60 K) v.19.0 (Bohao Biology Corp., Shanghai, China) in 2 to 5 μg of total RNA from SGC7901 cells before and after treatment with 2 μM and 4 μM 5-Aza-dC. Total RNA was extracted using TRIzol and miRNeasy mini kit (Qiagen, Hilden, Germany) according to the manufacturer's instructions. After measurement, the RNA samples were labeled using the miRNA Complete Labeling and Hyb kit (Agilent Technologies, Santa Clara, CA, USA). Scanning was performed using the Agilent Microarray Scanner and the raw intensity of the image was calculated using Gene Spring software 12.6.

Transient transfection. The miR-19a/b mimics or inhibitors and corresponding negative controls were designed and synthesized by Ambion (Guangzhou, China). Cells were plated at $2x10^5$ cells/well on 12-well plates with 1 ml of medium and were transfected at a final concentration of 10 μM using siPORT™ NeoFX™ transfection agent (Invitrogen) according to the manufacturer's protocols. Cells were collected 24 h after transfection.

Drug sensitivity assays. Log phase cells (5,000/well) were plated in 96-well plates and incubated under normal conditions. After 72 h, the sensitivity of GC cells to 5-fluorouracil (5-FU) and cisplatin (CDDP) was assessed using MTT assay. The concentration at which each drug produced 50% inhibition of growth (IC_{50}) was calculated as follows: $IgIC_{50} = Xm-I [P-(3-Pm-Pn)/4]$. Each experiment was performed in triplicate.

Cell apoptosis assays. After 24 h transfection, cells ($1x10^6$) were incubated with 5-FU and CDDP at a final concentration of 0.6 μg/ml for 48 h. Then, the cells were collected and cell apoptosis rate was detected using Annexin V-FITC Apoptosis Detection kit (BD Biosciences, Franklin Lakes, NJ, USA) according to the manufacturer's instructions. The data were analyzed using ModFit (BD Biosciences).

Western blot analysis. Cells were harvested at 72 h post-transfection and lysed in RIPA lysis buffer on ice. Immunodetection of MeCP2 was carried out with primary monoclonal antibody specific to MeCP2 (1:1,000; Abcam, Cambridge, MA, USA) and β-actin (1:3,000; Sigma, St. Louis, MO, USA) was used as control. The bands were scanned using the ChemiDocXRS + imaging system and quantified using Quantity One v4.6.2 software (both from Bio-Rad, Hercules, CA, USA). All experiments were performed in triplicate.

Luciferase reporter gene assays. Log phase cells were plated in 24-well plates for 12 to 20 h and were then transfected with 2 μg of MeCP2 3'-UTR luciferase reporter plasmids or empty pGL3-control vectors (Promega Biotech, Beijing, China) using Lipofectamine 2000 (Invitrogen). Cells were also co-transfected with miR-19a/b mimics (150 nM; Invitrogen). Forty-eight hours after transfection, assay was performed using the Dual-Luciferase® Reporter assay system (Promega

Biotech). The activities of firefly and Renilla luciferases were measured sequentially by adding LAR II and Stop and Glo® reagent. All experiments were performed in triplicate.

Immunohistochemistry. Immunohistochemistry was performed using paired GC and adjacent non-tumor gastric tissues microarray (Shanghai Outdo Biotech, Shanghai, China). Tissues were fixed in 10% formalin and paraffin-embedded. Sections were incubated with rabbit polyclonal anti-MeCP2 antibody (dilution 1:100; Santa Cruz Biotechnology, Inc., Santa Cruz, CA, USA) at 4°C overnight and then incubated with secondary antibody. Negative controls were incubated with rabbit IgG (Dako, Glostrup, Denmark). The intensity of staining was divided into four grades (intensity score): negative (0), weak (1), moderate (2) and strong (3). Positive rate was divided into five grades (percentage score): ≤1% (0), 2-25% (1), 26-50% (2), 51-75% (3), ≥75% (4). The histological scores were determined by the following formula: overall scores = percentage score x intensity score. An overall score was calculated and graded as negative (-, score <2), or positive (+, score ≥2).

In situ hybridization. The expression of miR-19a/b in paired GC and adjacent non-tumor gastric tissues microarray (Shanghai Outdo Biotech) was detected by *in situ* hybridization using probes for miR-19a/b (500 nmol) according to the manufacturer's protocol (Wuhan Boster, Wuhan, China).

Statistical analysis. Each experiment was repeated at least 3 times. Continuous data are presented as mean ± SEM and analyzed by Student's t-test. Categorical variables are presented as rate and are compared between two groups by Chi-square test. The linear correlation coefficient (Pearson's R) was calculated to determine the correlation between miR-19a/b and MeCP2 expression in GC tissues. All statistical analyses were performed using SPSS 17.0 software (SPSS, Inc., Chicago, IL, USA). $P<0.05$ or $P<0.01$ were considered to be statistically significant.

Results

miR-19a/b is upregulated in GC cells after 5-Aza-dC treatment. To test the effects of demethylation on GC cells, we treated SGC7901 cells with 2.5 μM demethylation reagent 5-Aza-dC. Then we found that the IC_{50} values of SGC7901 cells to 5-FU and CDDP were significantly increased by MTT assay ($P<0.01$) (Fig. 1A).

To further explore the miRNAs involved in the process, microarray analysis was performed in SGC7901 cells before and after 5-Aza-dC treatment. As shown in Fig. 1B, 38 and 25 miRNAs were found to be significantly upregulated (>2-folds increase) after 2.5 and 4 μM 5-Aza-dC treatments respectively. Among them, miR-19a/b increased most significantly. Quantitative RT-PCR results also showed that miR-19a/b mRNA levels increased significantly ($P<0.05$) (Fig. 1C). Then we transfected pre-miR-19a/b mimics and inhibitors, respectively into SGC7901 cells (Fig. 2A). As the results of MTT and flow cytometry assay showed, compared with negative control, IC_{50} values of SGC7901 cells to CDDP and 5-FU significantly increased ($P<0.05$) and similar tendency was also noted in cell apoptosis rate ($P<0.01$) (Fig. 2B and C) after mimics
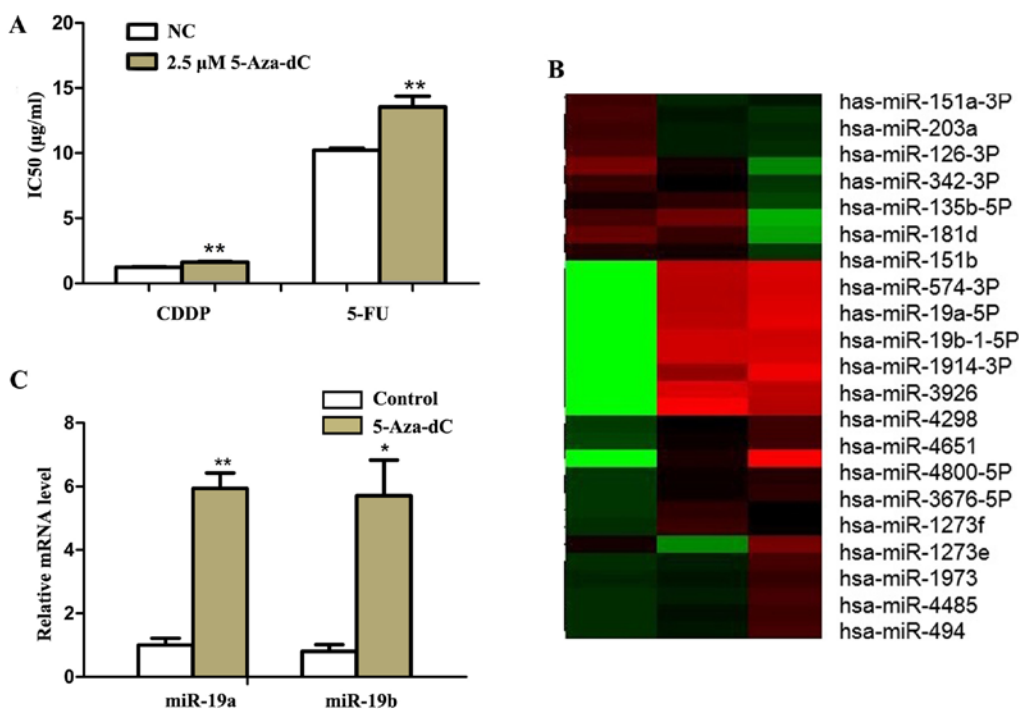
Figure 1. miR-19a/b is upregulated in SGC7901 cells by 5-aza-2'-deoxycytidine (5-Aza-dC) treatment. (A) IC_{50} values of SGC7901 cells to 5-fluorouracil (5-FU) and cisplatin (CDDP) were detected via MTT assay after treatment with 2.5 µM 5-Aza-dC for 72 h. (B) The expressions of mRNAs were analyzed by micro-array analysis after 2.5 and 4 µM 5-Aza-dC treatment for 72 h. (C) The expression of miR-19a and miR-19b were analyzed by qRT-PCR after 2.5 µM 5-Aza-dC treatment for 72 h. U6 was used as an internal control. Each experiment was repeated at least 3 times. *P<0.05 and **P<0.01.

transfection followed 5-Aza-dC treatment. Moreover, miR-19a/b knockdown had the opposite effect (P<0.01) (Fig. 3).

MeCP2 acts as a downstream target of miR-19a/b modulating MDR in GC cells after 5-Aza-dC treatment. Next, *in silico* analysis using miRanda and miRwalk showed that the 3'-UTR of MeCP2 contains three putative miR-19a/b binding sites. To validate the sites, the 3'-UTR of human MeCP2 was inserted downstream of the luciferase gene in the pGL3-control vector. Reporter gene assay showed that transfecting cells with pre-miR-19a/b mimics significantly decreased Luc-MeCP2 expression (Fig. 4A). Moreover, the transient transfection of SGC7901 cells with pre-miR-19a/b decreased MeCP2 protein level and miR-19a/b knockdown with inhibitors had the opposite effect by western blot assay (Fig. 4B).

To test the relationships between MeCP2 and MDR, we initially detected the expression levels of MeCP2 in SGC7901 cells and its MDR variants using western blot analysis. As shown in Fig. 5A, MeCP2 protein levels in SGC7901/VCR and SGC7901/ADR cells were significantly lower than in SGC7901 cells (P<0.01). Next, western blot results showed that MeCP2 expression was also significantly downregulated after 5-Aza-dC treatment (P<0.01) (Fig. 5A, right). Then we manipulated the expression of MeCP2 artificially. As shown in Fig. 5B, the MTT assay results showed that the IC_{50} value significantly decreased after transfection of MeCP2 expression vectors and knockdown of MeCP2 by siRNA had the opposite effect (P<0.01).

Further, to demonstrate the role of MeCP2 in miR-19a/b modulating MDR, SGC7901 cells were transfected with miR19a/b inhibitors and then treated with 2.5 and 4 µM 5-Aza-dC. Western blot results showed that MeCP2 protein

levels were significantly higher in miR-19a/b knockdown groups than in both control and 5-Aza-dC treatment groups (P<0.05) (Fig. 6).

MeCP2 modulates miR-19a/b in GC cell line after 5-Aza-dC treatment. To explore the effects of MeCP2 on miR-19a/b expression, we transfected MeCP2 siRNA or control into SGC7901 cells and then treated with 5-Aza-dC. MTT results showed that the IC_{50} value increased significantly after 5-Aza-dC treatment (P<0.01) and further increased after MeCP2 siRNA transfection (P<0.01) (Fig. 7A). In addition, miR-19a/b expression was significantly unregulated after MeCP2 knockdown following 5-Aza-dC treatment (P<0.01) (Fig. 7B).

miR-19a/b and MeCP2 are inversely correlated in GC tissues. We tested the expression of MeCP2 using immunohistochemistry, and the results showed that the expressions of MeCP2 were lower in GC tissues than in adjacent tissues (Fig. 8A). The positive rate of MeCP2 was 72.2 and 93.3% in GC and adjacent tissues (P<0.01). Then we performed *in situ* hybridization and found that expression of miR-19a and miR-19b was higher in GC tissues than in adjacent tissues (Fig. 8B). The positive rates in GC and in adjacent tissues were 82.8 vs. 70% and 92.2 vs. 72.2%, respectively (P<0.01). Furthermore, miR-19a and miR-19b were inversely correlated with MeCP2 expression by logistic regression analysis (P<0.05) (Fig. 8C). Finally, we analyzed the relationship between the expression of the molecules and clinicopathological parameters. The results showed that the positive rate of miR-19a was 92.5 vs. 60% in M0 and in M1 tissue samples (P<0.05) (Table I). However, no clinical parameters were significantly correlated with
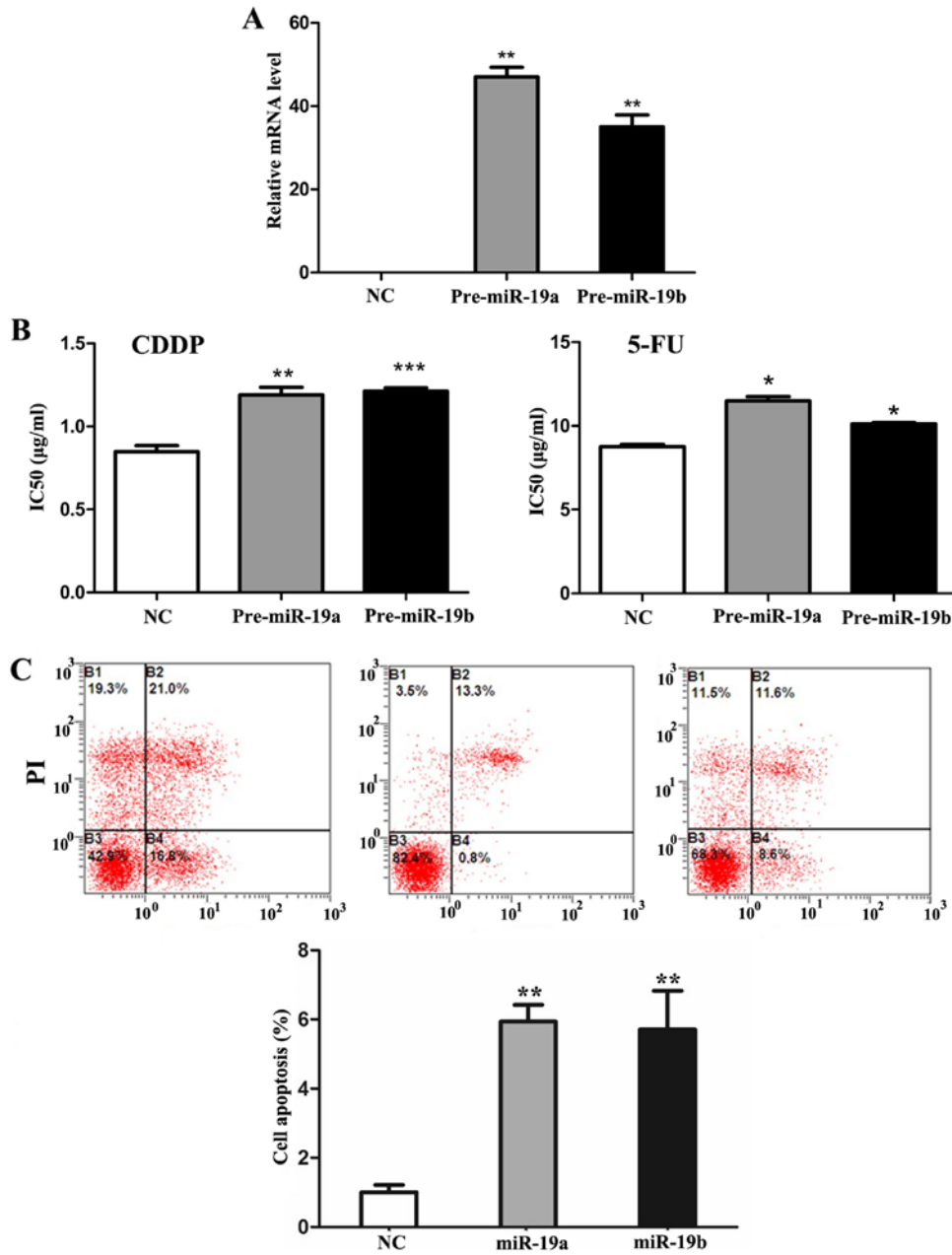
Figure 2. The effects of miR-19a/b transfection on multidrug resistance (MDR) in SGC7901 cells. (A) The mRNA expression levels of miR-19a/b after 24 h mimic transfection in SGC7901 cells by qRT-PCR. U6 was used as an internal control. (B) IC_{50} values of SGC7901 cells to 5-fluorouracil (5-FU) and cisplatin (CDDP) were detected via MTT assay after 24 h miR-19a/b mimic transfection. (C) Cell apoptosis rate was analyzed by flow cytometry analysis after 24 h miR-19a/b mimic transfection in SGC7901 cells. Each experiment was repeated at least 3 times. $^{*}P<0.05$ and $^{**}P<0.01$.
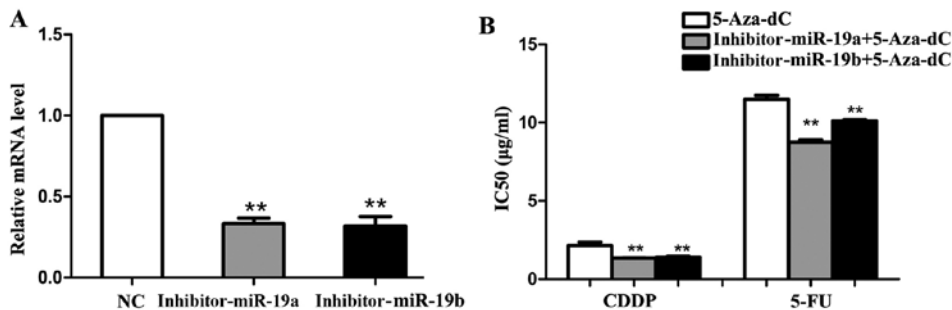

Figure 3. The effects of miR-19a/b knockdown on multidrug resistance (MDR) in SGC7901 cells. (A) The expression of miR-19a/b after 24 h inhibitor transfection were detected by qRT-PCR (U6 was used as an internal control). (B) IC_{50} values of SGC7901 cells to 5-fluorouracil (5-FU) and cisplatin (CDDP) were detected via MTT assay after 5-aza-2'-deoxycytidine (5-Aza-dC) treatment with or without miR-19a/b inhibitor transfection. Each experiment was repeated at least 3 times. $^{*}P<0.05$ and $^{**}P<0.01$.
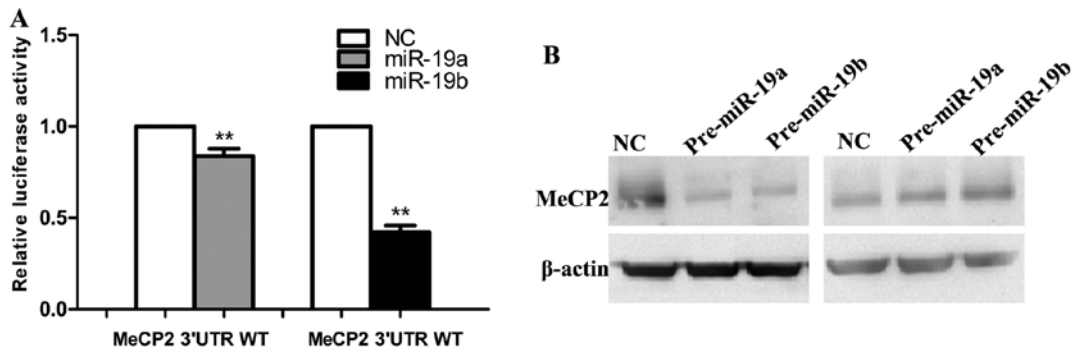
Figure 4. Methyl CpG binding protein 2 (MeCP2) acts as a direct target of miR-19a/b in SGC7901 cells. (A) Luciferase assays were performed with Luc-MeCP2 and Luc-NC following 48 h transfection with miR-19a/b mimics. (B) The expression of MeCP2 in SGC7901 cells was examined by western blotting after 72 h transfection with the miR-19a/b mimics and inhibitors. β-actin was used as control. Each experiment was repeated at least 3 times. $^*P<0.05$ and $^{**}P<0.01$.
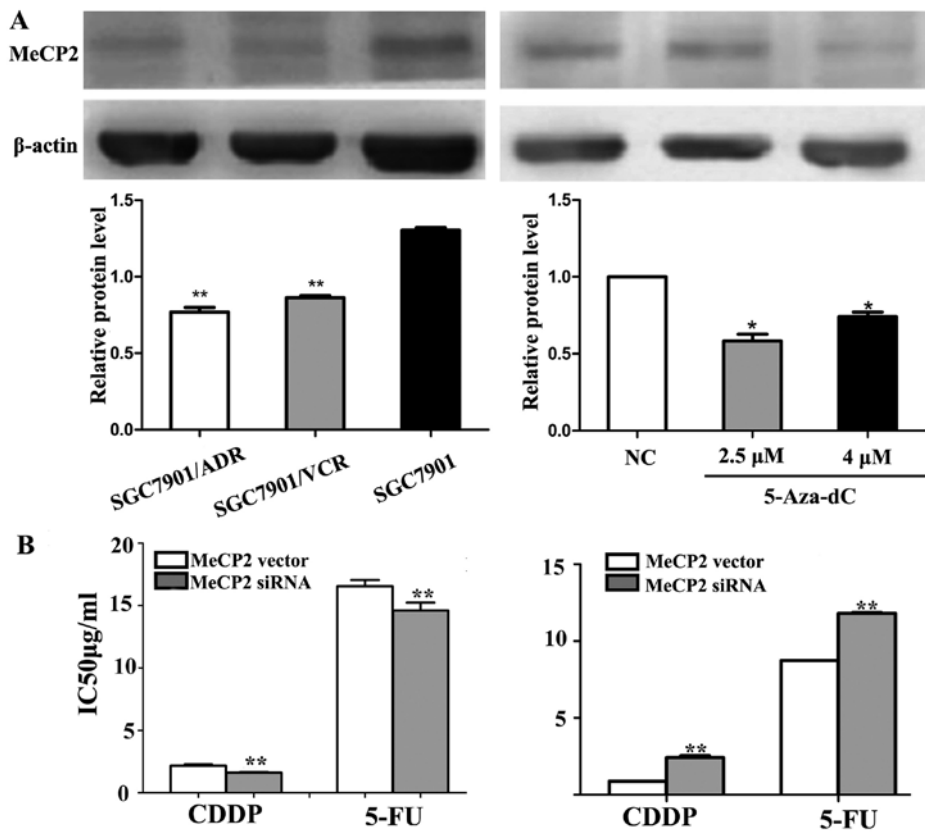

Figure 5. Methyl CpG binding protein 2 (MeCP2) modulates multidrug resistance (MDR) in SGC7901 cells. (A) Western blotting showed the expression of MeCP2 protein levels in SGC7901 cells and its MDR variants SGC7901/VCR and SGC7901/ADR. β-actin was used as control. (B) IC_{50} values of SGC7901 cells to 5-fluorouracil (5-FU) and cisplatin (CDDP) were detected via MTT assay after MeCP2 vector and siMeCP2 transfection. Each experiment was repeated at least 3 times. $^*P<0.05$ and $^{**}P<0.01$.
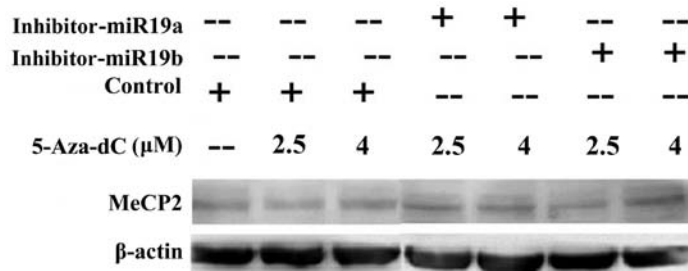

Figure 6. miR-19a/b regulates the expression of methyl CpG binding protein 2 (MeCP2) in 5-aza-2'-deoxycytidine (5-Aza-dC) induced multidrug resistance (MDR). After 2.5 and 4 μM 5-Aza-dC treatment, the expression of MeCP2 protein level was detected by western blotting with or without miR-19a/b inhibitors transfection. β-actin was used as control. $^*P<0.05$ and $^{**}P<0.01$.
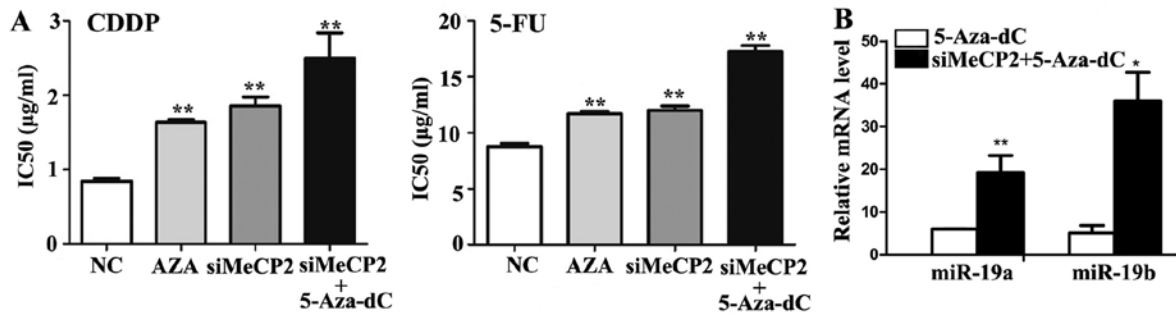
Figure 7. Methyl CpG binding protein 2 (MeCP2) represses the expression of miR-19a/b in SGC7901 cells. (A) IC$_{50}$ values of SGC7901 cells to 5-fluoro-uracil (5-FU) and cisplatin (CDDP) were detected via MTT assay after siMeCP2 transfection with or without 2.5 μM 5-aza-2'-deoxycytidine (5-Aza-dC) treatment. (B) The expression of miR-19a/b in SGC7901 cells was examined by western blotting after siMeCP2 transfection with or without 5-Aza-dC treatment. β-actin was used as control. Each experiment was repeated at least 3 times. *P<0.05 and **P<0.01.
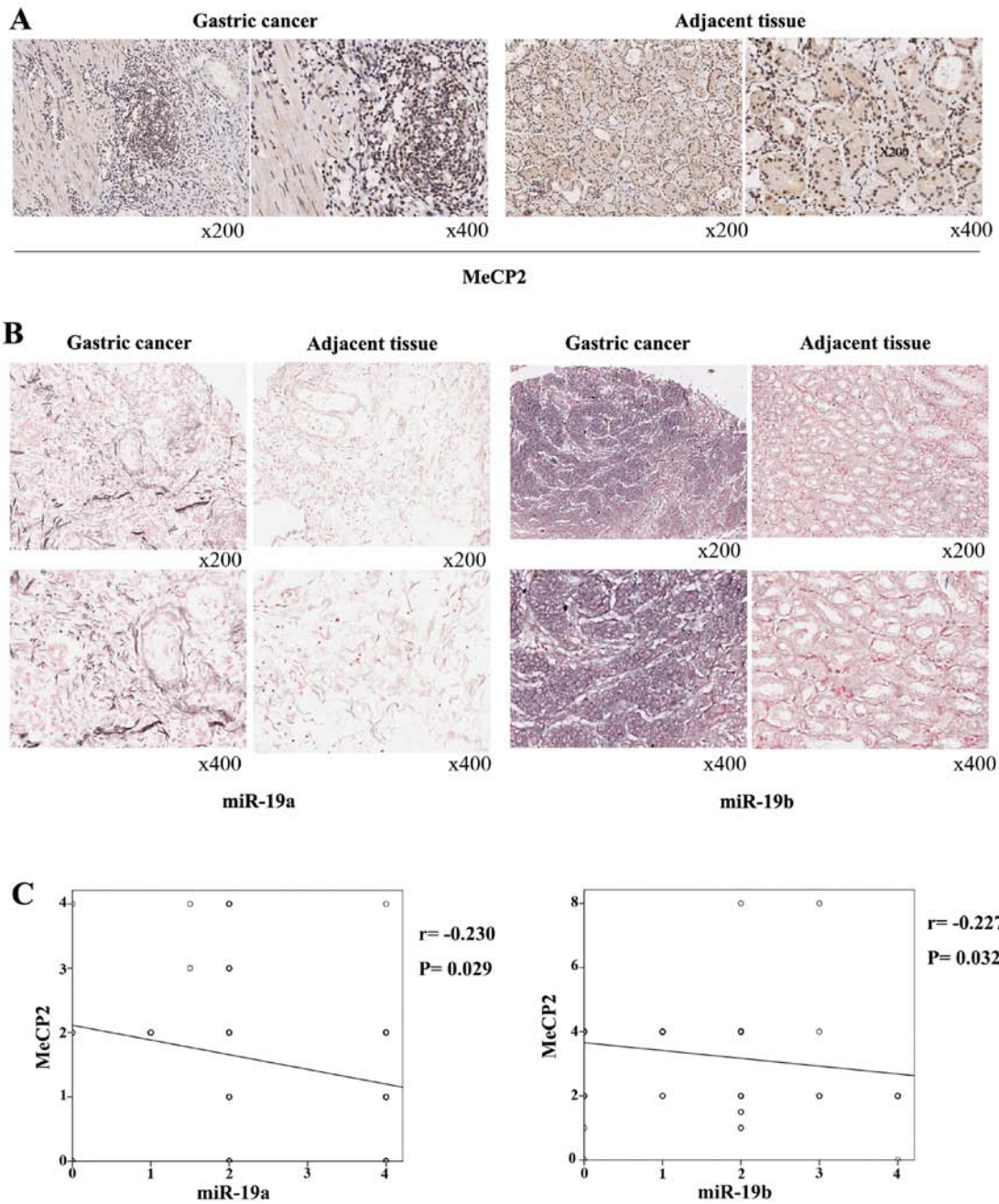
Figure 8. Methyl CpG binding protein 2 (MeCP2) is inversely correlated with miR-19a/b expression in gastric cancer (GC) tissues. (A) Immunohistochemistry analysis showed the expression of MeCP2 protein levels in GC tissues and adjacent tissues. (B) *In situ* hybridization analysis showed the expression of miR-19a/b levels in GC tissues and adjacent tissues. (C) The relationship between the expressions of miR-19a/b and MeCP2 was analyzed via logistic regression analysis.

Table I. The correlation between miR-19a and clinicopathological parameters.

	N	miR-19a Negative	miR-19a Positive	χ^2	P-value
Age (year)				0.003	0.956
≤60	34	5	29		
>60	56	16	40		
Sex				3.223	0.073
Male	60	6	54		
Female	30	7	23		
Tumor diameter (cm)				0.690	0.690
≤5	53	7	46		
>5	37	6	31		
TNM				0.655	0.384
I+II	37	5	32		
III+IV	53	9	44		
Lymph node metastasis				1.431	0.698
N0	22	2	20		
N1	18	4	14		
N2	23	3	20		
N3	27	4	23		
Distant metastasis				5.945	0.01
M0	80	9	71		
M1	10	4	6		

Table II. The correlation between miR-19b and clinicopathological parameters.

	N	miR-19b Negative	miR-19b Posisive	χ^2	P-value
Age (year)				1.521	0.218
≤60	34	1	33		
>60	56	6	50		
Sex				0.310	0.578
Male	60	4	56		
Female	30	3	27		
Tumor diameter (cm)				0.010	0.922
≤5	53	4	49		
>5	37	3	34		
TNM				0.493	0.483
I+II	37	2	35		
III+IV	53	5	48		
Lymph node metastasis				0.885	0.650
N0	22	1	21		
N1	18	2	16		
N2	23	2	21		
N3	27	2	25		
Distant metastasis				0.077	0.781
M0	80	6	74		
M1	10	1	9		

miR-19b expression (Table II). The positive rate of MeCP2 was 83.8 vs. 64.2% in phase I + II patients and phase III + IV patients (P<0.05), 86.7 vs. 48.3% in female and male patients (P<0.05), and 68.8 vs. 100% in M0 and M1 tissue samples (P<0.05) (Table III).

Discussion

Our and others previous studies have demonstrated that aberrant expression of miRNAs was involved in the development of MDR in GC (2,11,12). As the most significant miRNAs of the miR-17-92 cluster, miR-19a/b was identified to be potential oncogene in GC (13). We have found that miR-19a/b can regulate the self-renewal of GC stem cells (14), promote metastasis (15), and also sustain the MDR of GC cells (12). However, the potential mechanisms have not been fully clarified.

Epigenetics, mainly including DNA methylation and histone modification, have been recognized as important factors in regulating cancer MDR (2,16,17). Demethylation of the MDR1 promoter was found to be strongly associated with the acquisition of MDR phenotype through decreasing drug accumulation (18). Likewise, demethylation of the hMLH1 promoter by DNMT1 restores mismatch repair proficiency and drug sensitivity to 5-FU in colorectal cancer cells (19). In addition, DNA hypermethylation of miR-199b-5p is frequently

silenced and mediates acquired chemoresistance in ovarian cancer (20). All these studies indicate that demethylation is a crucial regulatory mechanism in cancer MDR phenotype. Previous study indicated that DNA methylation silences the expression of miR-17-92 cluster in lung tissue and fibroblast cell lines of IPF patients (10). So we hypothesized that demethylation of miR-19a/b could result in gene upregulation and promote MDR in GC. As expected, demethylation agent 5-Aza-dc treatment increased the expression of miR-19a/b and accelerated the development of MDR. Furthermore, *in vitro* experiments using deletion-reintroduction cell models demonstrated that miR-19a/b directly modulated the development of acquired drug resistance. All these results indicated that hypomethylation of miR-19a/b is a pivotal molecular mechanism in gene regulation and is consistent with our previous studies that the miR-19a/b acts as an oncomiR in GC (12,14,15).

MeCP2 is the first discovered and best studied MBD, which contains a MBD domain binding to methylated CpG dinucleotides and a transcriptional repression domain (TRD) interacting with histone deacetylase. So MeCP2 is important in coordinating crosstalk between methylation, histone modifications and chromatin organization to achieve an integral transcriptional program (21). Loss of function mutations can result in Rett syndrome (22). Besides, aberrations MeCP2 proteins expressions have also been implicated in many

Table III. The correlation between MeCP2 and clinicopathological parameters.

		MeCP2			
	N	Negative	Positive	χ^2	P-value
Age (year)				0.047	0.829
≤60	34	9	25		
>60	56	16	40		
Sex				4.680	0.031
Male	60	21	39		
Female	30	4	26		
Tumor diameter (cm)				0.119	0.730
≤5	53	14	39		
>5	37	11	26		
TNM				4.186	0.041
I+II	37	6	31		
III+IV	53	19	34		
Lymph node metastasis				0.938	0.061
N0	22	4	18		
N1	18	5	13		
N2	23	8	15		
N3	27	8	19		
Distant metastasis				4.327	0.038
M0	80	25	55		
M1	10	0	10		

cancers (23). Previously, El-Osta et al reported that MeCP2 is involved in methylation-dependent silencing of human MDR1 in CES cells (24). In this study we demonstrated that MeCP2 was a target of miR-19a/b. These data indicate that MeCP2 may be directly involved in MDR process.

However, our results indicated that the positive rate of MeCP2 was higher in adjacent tissues than in GC tissues, which is inconsistent with previous results (25,26). The discrepancy maybe due to the different clinical characteristics of patients. Although Wada et al reported that MeCP2 expression was higher in intestinal-type GC tissues than in adjacent tissues, no similar tendency was observed in diffuse-type GC. In addition, higher MeCP2 expression in GC tissues were observed in only 43.8% patients (25). In the study of Tong et al, no clinicopathological information was provided and 90.5% of patients were male (26). Our results in this study showed that the positive rate of MeCP2 expression was significantly higher in female patients. So patients' sex may affect MeCP2 expression. However, our results indicated that the positive rate of MeCP2 expression was significantly higher in M1 patients than in M0 patients. So the role of MeCP2 in GC as an oncogene or antioncogene is complicated and needs further studies.

Interestingly, we found that downregulating MeCP2 could increase 5-Aza-dc induced miR-19a/b expression. We further confirmed the inverse correlation between miR-19a/b and MeCP2 in GC tissues. Although the molecular mechanisms necessary for repression miR-19a/b expression require further studies, our results clearly indicate a unique coordinating regulatory feedback circuits between miR-19a/b and MeCP2 in modulating MDR process. These results show that methylation not only directly regulates miRNAs expression, but also acts as an important mechanism mediating the roles of MBPs in MDR process.

In conclusion, our results revealed that demethylation of miR-19a/b repress MeCP2 expression via direct binding at the 3'-UTRs, which then alleviates the inhibitor effects of MeCP2 on miR-19a/b expression. Thus, the autoregulatory network sustains the preservation of the expression levels of miR-19a/b and plays an important role in GC MDR.

Availability of data and material

All data are provided in full in the results section of this paper.

Authors' contributions

FZ, QW and YS conceived and designed the study. FZ, QW, CL and TL performed the experiments. FZ and ZN analysed the results. QW and ZN wrote the paper. ZN and YS reviewed and edited the manuscript. All authors read and approved the final manuscript.

Ethics approval and consent to participate

The study was approved by the Institutional Review Board of Xijing Hospital. All patients provided written informed consent.

Consent for publication

Not applicable.

Competing interests

The authors declare that they have no competing interests.

References

1. Allemani C, Weir HK, Carreira H, Harewood R, Spika D, Wang XS, Bannon F, Ahn JV, Johnson CJ, Bonaventure A, et al; CONCORD Working Group: Global surveillance of cancer survival 1995-2009: Analysis of individual data for 25,676,887 patients from 279 population-based registries in 67 countries (CONCORD-2). Lancet 385: 977-1010, 2015.
2. Wu Q, Yang Z, Nie Y, Shi Y and Fan D: Multi-drug resistance in cancer chemotherapeutics: Mechanisms and lab approaches. Cancer Lett 347: 159-166, 2014.

3. Hashimoto Y, Akiyama Y and Yuasa Y: Multiple-to-multiple relationships between microRNAs and target genes in gastric cancer. PLoS One 8: e62589, 2013.
4. Guo X, Xia J and Yan J: Promoter methylated microRNAs: Potential therapeutic targets in gastric cancer. Mol Med Rep 11: 759-765, 2015.
5. Olive V, Bennett MJ, Walker JC, Ma C, Jiang I, Cordon-Cardo C, Li QJ, Lowe SW, Hannon GJ and He L: miR-19 is a key oncogenic component of mir-17-92. Genes Dev 23: 2839-2849, 2009.
6. Olive V, Jiang I and He L: mir-17-92, a cluster of miRNAs in the midst of the cancer network. Int J Biochem Cell Biol 42: 1348-1354, 2010.
7. Woods K, Thomson JM and Hammond SM: Direct regulation of an oncogenic micro-RNA cluster by E2F transcription factors. J Biol Chem 282: 2130-2134, 2007.
8. Tili E, Michaille JJ, Liu CG, Alder H, Taccioli C, Volinia S, Calin GA and Croce CM: GAM/ZFp/ZNF512B is central to a gene sensor circuitry involving cell-cycle regulators, TGF{beta} effectors, Drosha and microRNAs with opposite oncogenic potentials. Nucleic Acids Res 38: 7673-7688, 2010.
9. Dews M, Homayouni A, Yu D, Murphy D, Sevignani C, Wentzel E, Furth EE, Lee WM, Enders GH, Mendell JT, et al: Augmentation of tumor angiogenesis by a Myc-activated microRNA cluster. Nat Genet 38: 1060-1065, 2006.
10. Dakhlallah D, Batte K, Wang Y, Cantemir-Stone CZ, Yan P, Nuovo G, Mikhail A, Hitchcock CL, Wright VP, Nana-Sinkam SP, et al: Epigenetic regulation of miR-17~92 contributes to the pathogenesis of pulmonary fibrosis. Am J Respir Crit Care Med 187: 397-405, 2013.
11. Wu Q, Yang Z, Xia L, Nie Y, Wu K, Shi Y and Fan D: Methylation of miR-129-5p CpG island modulates multi-drug resistance in gastric cancer by targeting ABC transporters. Oncotarget 5: 11552-11563, 2014.
12. Wang F, Li T, Zhang B, Li H, Wu Q, Yang L, Nie Y, Wu K, Shi Y and Fan D: MicroRNA-19a/b regulates multidrug resistance in human gastric cancer cells by targeting PTEN. Biochem Biophys Res Commun 434: 688-694, 2013.
13. Guo J, Miao Y, Xiao B, Huan R, Jiang Z, Meng D and Wang Y: Differential expression of microRNA species in human gastric cancer versus non-tumorous tissues. J Gastroenterol Hepatol 24: 652-657, 2009.
14. Wu Q, Yang Z, Wang F, Hu S, Yang L, Shi Y and Fan D: MiR-19b/20a/92a regulates the self-renewal and proliferation of gastric cancer stem cells. J Cell Sci 126: 4220-4229, 2013.
15. Wu Q, Yang Z, An Y, Hu H, Yin J, Zhang P, Nie Y, Wu K, Shi Y and Fan D: MiR-19a/b modulate the metastasis of gastric cancer cells by targeting the tumour suppressor MXD1. Cell Death Dis 5: e1144, 2014.
16. Wang X, Gao H, Ren L, Gu J, Zhang Y and Zhang Y: Demethylation of the miR-146a promoter by 5-Aza-2'-deoxycytidine correlates with delayed progression of castration-resistant prostate cancer. BMC Cancer 14: 308, 2014.
17. Liu J, Zhang X, Liu A, Zhang D, Su Y, Liu Y, You D, Yuan L, Kong X, Wang X, et al: Altered methylation of glucosylceramide synthase promoter regulates its expression and associates with acquired multidrug resistance in invasive ductal breast cancer. Oncotarget 7: 36755-36766, 2016.
18. Chen KG and Sikic BI: Molecular pathways: Regulation and therapeutic implications of multidrug resistance. Clin Cancer Res 18: 1863-1869, 2012.
19. Fang JY, Lu R, Mikovits JA, Cheng ZH, Zhu HY and Chen YX: Regulation of hMSH2 and hMLH1 expression in the human colon cancer cell line SW1116 by DNA methyltransferase 1. Cancer Lett 233: 124-130, 2006.
20. Liu MX, Siu MK, Liu SS, Yam JW, Ngan HY and Chan DW: Epigenetic silencing of microRNA-199b-5p is associated with acquired chemoresistance via activation of JAG1-Notch1 signaling in ovarian cancer. Oncotarget 5: 944-958, 2014.
21. Neupane M, Clark AP, Landini S, Birkbak NJ, Eklund AC, Lim E, Culhane AC, Barry WT, Schumacher SE, Beroukhim R, et al: MECP2 is a frequently amplified oncogene with a novel epigenetic mechanism that mimics the role of activated RAS in malignancy. Cancer Discov 6: 45-58, 2016.
22. Du Q, Luu PL, Stirzaker C and Clark SJ: Methyl-CpG-binding domain proteins: Readers of the epigenome. Epigenomics 7: 1051-1073, 2015.
23. Sansom OJ, Maddison K and Clarke AR: Mechanisms of disease: Methyl-binding domain proteins as potential therapeutic targets in cancer. Nat Clin Pract Oncol 4: 305-315, 2007.
24. El-Osta A, Kantharidis P, Zalcberg JR and Wolffe AP: Precipitous release of methyl-CpG binding protein 2 and histone deacetylase 1 from the methylated human multidrug resistance gene (MDR1) on activation. Mol Cell Biol 22: 1844-1857, 2002.
25. Wada R, Akiyama Y, Hashimoto Y, Fukamachi H and Yuasa Y: miR-212 is downregulated and suppresses methyl-CpG-binding protein MeCP2 in human gastric cancer. Int J Cancer 127: 1106-1114, 2010.
26. Tong D, Zhao L, He K, Sun H, Cai D, Ni L, Sun R, Chang S, Song T and Huang C: MECP2 promotes the growth of gastric cancer cells by suppressing miR-338-mediated antiproliferative effect. Oncotarget 7: 34845-34859, 2016.